Synchronous scanning of undulator gap and monochromator for XAFS measurements in soft x-ray region

Tomoaki Tanaka,[a*] Nobuyuki Matsubayashi,[a] Motoyasu Imamura[a] and Hiromichi Shimada[a]

[a]*National Institute of Material and Chemical Research, Tsukuba, Ibaraki 305-8565, Japan.*
Email:tanakat@nimc.go.jp

Synchronous scanning of the undulator gap and a monochromator was done to obtain smooth profiles of incident x-rays that are suitable for XAFS measurements. By changing the gap from 150 mm (B=0.12 T) to 140 mm (B=0.15 T) with the use of the 3rd to 11th harmonic peaks, soft x-rays with energy from 200 eV to1200 eV were obtained. The smooth profile of the incident x-rays provided high-quality measurement of XANES and EXAFS spectra in the soft x-ray region. Issues that would improve the synchronous scanning system are discussed.

Keywords; undulator, synchronous scan, soft x-ray

1. Introduction

An undulator light source has excellent properties as an x-ray excitation probe. These properties, such as high brilliance and quasi-monochromatic energy spectrum, are useful when the source is used as a probe for photoemission that does not require the scanning of the photon energy. In contrast, the characteristic spectra of undulators with intense harmonic peaks often result in serious problems for XAFS measurements with wide energy ranges, because I_0 correction (dividing signals from the sample by the intensity of incident x-rays) is not effective due to nonlinear response of detectors or interference with higher-order diffraction photons.

The synchronous scanning of the undulator gap and a monochromator is the best method for overcoming the above problems and for maximizing the characteristics of undulators in XAFS measurements. In the hard x-ray region, for QEXAFS measurements the undulator gap of ID26 in ESRF was previously scanned at a constant speed with a synchronous movement of a double crystal monochromator (Solé et al., 1999). Synchronous scan should be useful also in the soft x-ray region that needs diffraction grating monochromator; however, very few studies have been reported. In our current study, for the soft x-ray region (200-1200 eV), we did synchronous scans of a monochromator (diffraction grating and exit slit) and the undulator gap of the BL13C (Matsubayashi et al., 1992, Shimada et al. 1995) of the Photon Factory located in Tsukuba City, Japan.

2. Experimental

2.1 Apparatus

The BL13 of the Photon Factory is equipped with a 27-pole wiggler/undulator that is designed for both modes of wiggler and undulator (Kitamura et al., 1989). For soft x-ray experiments at BL13C, the insertion device is used as an undulator (weak magnetic field), whereas for hard x-ray experiments at BL13A and BL13B, it is used as a multi-pole wiggler (strong magnetic field). The BL13C was designed based on the cylindrical element monochromator (CEM) concept (Chen and Sette, 1989) and is equipped with three laminar-type gratings of 350, 750, and 1500 gr./mm that covers a photon energy range of 80-1500eV.

2.2 Scan of the undulator gap

At the BL13C, the highest photon energy of the fundamental harmonic is 310 eV when the undulator gap is fully open (248 mm, B=0.02 T). Thus, higher-order harmonic peaks must be used to cover the soft x-ray region. In our experiments, small undulator gaps with high magnetic fields were avoided, because the resulting high heat load would fatally damage the optical elements. Large changes in the undulator gap over a short period of time were also avoided, because rapid changes in the heat load cause unstable photon energy or photon flux at the sampling position. For instance, when the gap was decreased from 200 mm (B=0.05 T) to 125 mm (B=3.36 T), the total photon power (P) increased from 6 W to 100 W. This large change in the heat load could not be completely compensated in a short period by the cooling system of the BL13C. Considering these conditions, we chose the range of undulator gap between 140 mm (B=0.15 T, P=56 W) and 150 mm (B=1.2 T, P=38 W) to obtain a photon energy from 200 eV to 1200 eV that covers K-edges of C, N, O, and F and L-edges of most of the first-row transition metals.

Figure 1 shows the undulator spectra of the 150-mm and 140-mm gaps with the harmonic peaks used in the synchronous scan mode. Table 1 summarizes the order of harmonic peaks corresponding to the photon energy. The undulator gap at each photon energy was calculated by using a third polynomial fitting to the experimentally obtained optimum gap values, and was changed by a minimum step of 0.01 mm.

Figure 2 shows a flow diagram of the undulator gap scanning procedure. First, the optimum undulator gap corresponding to the required photon energy was calculated and compared with the present gap. When the difference (△) between the calculated gap and

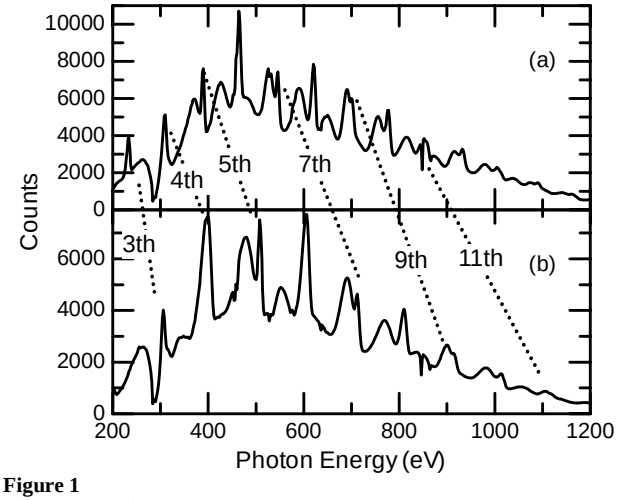

Figure 1
Undulator profiles for (a) 140mm gap and (b)150mm gap. Dotted lines indicate the order of harmonics. The spectra were obtained by monitoring the total electron yield.

Table 1
Photon energy and order of harmonic used for synchronous scan

Photon energy (eV)	200-310	310-400	400-520	520-700	700-900	900-1200
Order of harmonics	3rd	4th	5th	7th	9th	11th

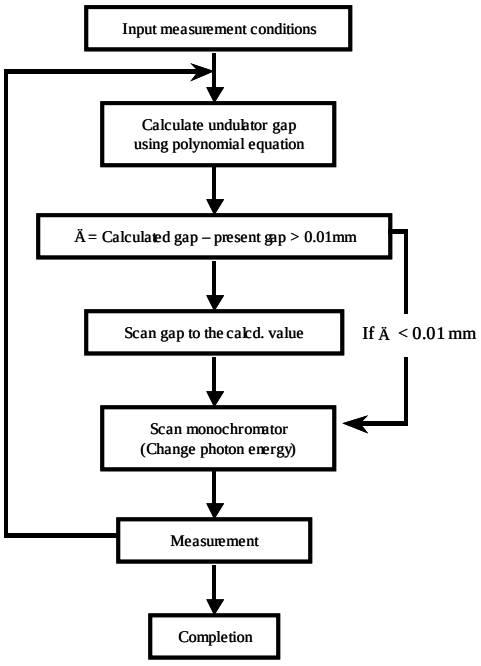

Figure 2
Diagram of the undulator gap scan procedure

present gap was larger than 0.01 mm, the undulator gap was changed to the calculated value, whereas when $\triangle$<0.01 mm, the gap was not changed. All of the above procedures were done by using a PC (placed at the beam line) that was connected to the central computer of the storage ring that controls the undulator gap of the BL13C. After the gap was changed, this central computer sent a command to another PC that controls the grating and exit slit position of the BL13C, to change the photon energy. Because about five seconds is needed to change the undulator gap, it is not practical to scan the undulator gap in XAFS measurements of narrow energy regions.

3. Results

3.1 C K-edge XANES

Figure 3a shows the profile of incident x-ray intensities at the C K-edge. The solid line is the spectrum obtained by synchronous scanning of the undulator gap and the monochromator, and the dotted line is the spectrum for a 160-mm gap. The structures between 280eV and 295eV were caused by the absorption by carbon deposited on the optical elements, most likely on the grating, and thus could not be avoided. The structure due to the deposited carbon was seemingly enhanced when the undulator gap was synchronously scanned. Nevertheless, the effect of the structures was eliminated by the I_0 correction, as shown by the solid line in the C K-edge spectrum of graphite in Fig. 3b, because the signal-to-background ratio was sufficiently high in this case.

3.2 C K-edge EXAFS

As compared with a XANES analysis, an EXAFS analysis requires more accurate I_0 correction of absorption spectra, because EXAFS analyzes small oscillations on relatively high background that span wide energy regions. Thus, synchronous scanning that gives smooth I_0 profiles plays a more important role in an EXAFS analysis than in a XANES analysis.

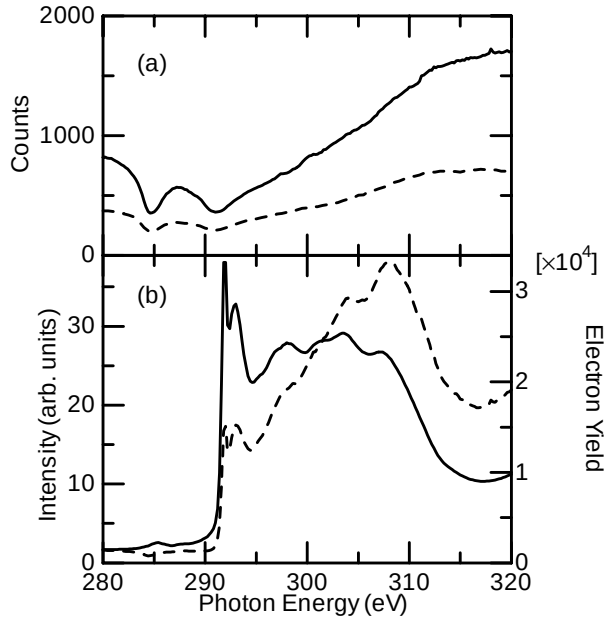

Figure 3
(a) Incident X-ray intensity I_0 at C K-edge; synchronous scan of undulator gap and monochromator (solid line), and of fixed gap at 160mm (dotted line).
(b) C K-edge x-ray absorption spectra (XANES region) of graphite after I_0 correction (solid line) and before correction (dotted line).

Figure 4a gives the C K-edge absorption spectrum of graphite after I_0 correction measured by the synchronous scanning. Although the spectrum shows some inflections, the overall profile in the EXAFS region was relatively monotonous, showing that the I_o correction was effective. Figure 4b shows the EXAFS oscillation, $\chi(k)$, after subtracting the background. The spectrum might include some ghost oscillations due to the interference with higher-order photons. Fig. 4c shows the radial distribution profile obtained by Fourier transformation of the k/f(k) weighted $\chi(k)$. The first peak at 0.133 nm was due to the first-neighbor C-C scattering (0.142 nm, N=3). The second peak at 0.247 nm, which could not be resolved, included contributions from the second-neighbor (0.246 nm, N=6) and third-neighbor (0.284 nm, N=3) carbon atoms. The third peak at 0. 387 nm was likely due to the fourth-neighbor C-C scattering (0.376 nm, N=6). These results are consistent with previous results by Comelli (1988).

4. Discussion and summary

We presented a synchronous scanning system for the undulator gap and the monochromator of the BL13C of the Photon Factory. The system functioned satisfactorily for C K-edge XANES and C K-edge EXAFS measurements. The method was effective also for photoemission experiments, including resonant photoemission measurements, because the users of the beam line were able to obtain high-intensity soft x-rays without special knowledge on the beam line performance, such as undulator spectra profiles.

Certain issues still need to be resolved. For example, the contamination from the higher order harmonics should be minimized by introducing a cut-off mirror at the end of the beam line. Because the undulator gap of BL13 cannot be scanned continuously and synchronously with the monochromator as has been done at ESRF (Solé et al., 1999), the dead time for changing the gap cannot be avoided. However, the present dead time (about five seconds for a

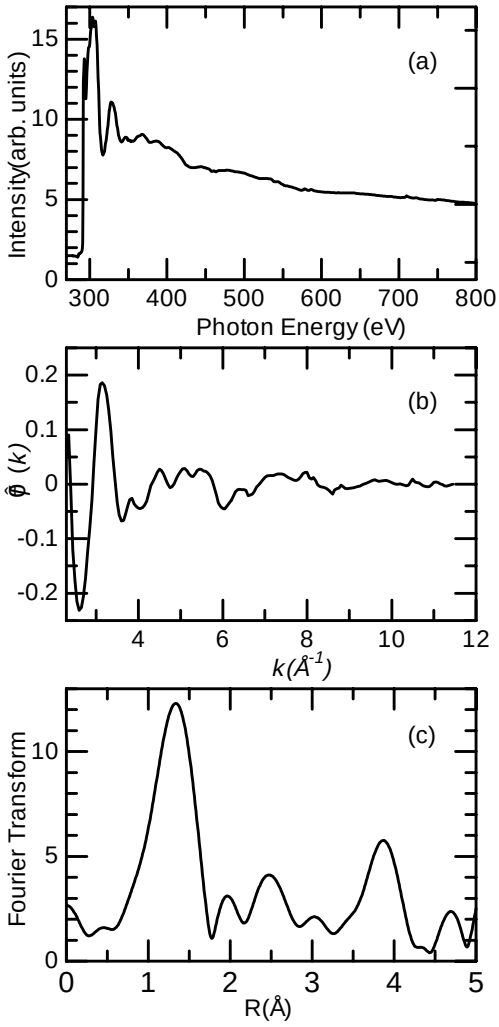

Figure 4
(a) C K-edge x-ray absorption spectrum (EXAFS region) of graphite after I_0 correction (b)EXAFS oscillation of graphite (c)Fourier transform result of (b).
(The acquisition time is 1 sec/pts for XANES and EXAFS measurements.)

step) should be significantly shortened particularly for XANES and EXAFS measurements because the acquisition time for each photon energy is relatively short relative to the dead time. Further collaboration with the staff responsible for the insertion device is needed to confirm this.

5. Acknowledgement

We appreciate the collaboration with the staff responsible for the insertion device at the Photon Factory. The experiments were done under the approval of the Photon Factory Program Advisory Committee (Proposal 99PF-14).

Reference

Chen, C. T. & Sette, F. (1989). Rev. Sci. Instrum. **60**(7), 1616-1621.
Comelli, G., Stöhr, J. & Jark W. (1988). Phys. Rev. B **37**(9), 4383-4389.
Kitamura, H., Yamamoto, S. & Kamada, S. (1989). Rev. Sci. Instrum. **60**(7), 1407-1413.
Matsubayashi, N., Shimada, H., Tanaka, K., Sato, T., Yoshimura, Y. & Nishijima, A. (1992). Rev. Sci. Instrum. **63**(1), 1363-1366.
Shimada, H., Matsubayashi, N., Imamura, M., Sato, T., Yoshimura, Y., Hayakawa, T., Takehira, K., Toyoshima, A., Tanaka, K. & Nishijima, A. (1995). Rev. Sci. Instrum. **66**(2), 1780-1782.
Solé, V. A., Gauthier, C., Goulon, J. & Natali, F. (1999). *J. Synchrotron Rad.* **6**, 174-175.